Polyvinyl chloride (PVC) derived microporous carbons prepared via hydrothermal dechlorination and potassium hydroxide activation for efficient CO_2 capture

Fangming Yang [a, b], *Xin Liu* [b*], *Mengbin Li* [b], *Clement Uguna* [b], *Wenlong Wang* [a], *Chenggong Sun* [b*]

a School of Energy and Power Engineering, Shandong University, Jinan, PR China

b Faculty of Engineering, University of Nottingham, Nottingham NG7 2RD, UK

Abstract

Hydrothermal dechlorination has been widely studied for recycling end-of-life polyvinyl chloride while the impact of embedded metal additives, a major component of many waste PVC products, has rarely been reported. In this study, hydrothermal treatment of used polyvinyl chloride pipe was carried out at a temperature range between 220 and 280 °C to understand the role of metal additives in the dechlorination process. The potential application of chlorine-free hydrochar as the precursor to prepare CO_2 sorbents via chemical activation was also evaluated. The results demonstrated that the well-distributed calcium carbonate in the polyvinyl chloride matrix, acting as an in-situ neutralization agent, could accelerate the dechlorination of PVC, over 98.4% of chlorine was removed at 260 °C or higher. Using the hydrochar prepared at 260 °C as a single precursor, a series of activated carbons were successfully prepared via a facile chemical activation process. Those hydrochar-derived carbons have a microporous dominant structure with high surface area and total pore volume reaching up to 1927 $m^2 g^{-1}$ and 0.85 $cm^3 g^{-1}$, which showed great potential as CO_2 sorbents. Tested at 25 °C, the microporous carbons exhibited both remarkable CO_2 adsorption capacities of 1.60 mmol g^{-1} and 4.05 mmol g^{-1} at 100 kPa and high CO_2/N_2 selectivity of 42 at 15 kPa CO_2. Advanced characterization demonstrated that the excellent CO_2 adsorption performance originated from a unique combination of ultra-microporosity and surface chemistry. This work provides an effective and sustainable strategy to recycle hard-to-handle chlorinated plastic waste and reduce carbon emission.

Highlights

- Hydrothermal treatment of PVC containing additives (20 wt%) was carried out.
- The in-situ $CaCO_3$ could accelerate the dechlorination of PVC under mild conditions.
- Microporous carbons were successfully prepared by using PVC derived hydrochar.
- HPVC carbons exhibit superior CO_2 uptake and CO_2/N_2 selectivity at 25 °C.

Key words: hydrothermal dechlorination, plastic recycling, hydrochar, microporous carbon, carbon capture

Word Count: 7849 words

---

* Corresponding author.

E-mail addresses: xin.liu@nottingham.ac.uk (X. Liu), cheng-gong.sun@nottingham.ac.uk (C. Sun)

Nomenclature

Abbreviations

PVC
polyvinyl chloride

XRF
X-ray fluorescence spectroscopy

NLDFT
non-local density functional theory

FEI-SEM
field-emission scanning electron microscope

DSL
dual-site Langmuir

PSD
pore size distribution

BET
Brunauer–Emmett–Teller theory

IAST
ideal adsorption solution theory

Symbols

Cl_{PVC}
concentration of chlorine in original PVC

$Cl_{product,\ T}$
concentration of chlorine in hydrochar at hydrothermal temperature of T

T
hydrothermal temperature

Y_{T}
yield of hydrochar at hydrothermal temperature of T

q
adsorption capacity

q_A
mono-layer CO_2 capacity of site A

q_B
mono-layer CO_2 capacity of site B

p
equilibrium pressure

b_A
adsorption equilibrium constants for site A

b_B
adsorption equilibrium constants for site B

$\mathrm{S}_{\mathrm{BET}}$
BET surface area

$\mathrm{V}_{\mathrm{total}}$
total pore volume

$\mathrm{V}_{\mathrm{micro}}$

micropore volume

$V_{micro<0.7nm}$

volume of pores <0.7 nm

Q_{st}

isosteric heat of CO_2 adsorption

1.0 Introduction

Polyvinyl chloride (PVC), one of the most commonly used and also most environmentally damaging plastic, has been widely used in building, construction and packaging due to its unique advantages including high durability, reusability and low thermal conductivity [1−3]. According to the Plastics Europe report, the demand for PVC reached 4.7 Mt in Europe, accounting for 9.6% of the total plastic demand, which is only lower than polyethylene (PE) and polypropylene (PP) [4]. So, the recycling of end-of-life PVC is receiving increasing attention. However, its high chlorine content (around 56 wt% of the polymer's weight) and high levels of hazardous additives become the major barrier to recycling end-of-life PVC. Under the current condition, landfill and incineration are the two main approaches for the disposal of waste PVC. Landfill of PVC leads to the formation of Cl-containing hazards during photodegradation that could migrate to the soil, water and atmosphere while the formation of hydrochloric acid (HCl) and dioxin become the major barriers to its efficient recycling processes such as incineration or pyrolysis [5 ,6]. Therefore, there is an urgent need for a safe and environmentally friendly approach to waste management of end-of-life PVC.

Dechlorination before treatment has been considered as an essential step for recycling PVC waste. Several methods including dehalogenation using NaOH and KOH/organic solvent mixture, ionic liquid (IL) mediated dehydrochlorination, thermal treatment and hydrothermal treatment have been developed [2, 7−10]. Although the high dehalogenation could be achieved at room temperature, dehalogenation using organic NaOH or KOH solution is a complicated process and organic solvents such as DMF are of great environmental concern [11]. ILs also suffer from high cost, toxicity in living organisms and inferior biodegradability [12]. In comparison, hydrothermal treatment is increasingly recognized as a reliable, safe and environmentally friendly approach for PVC dechlorination whilst the final product, chlorine-free hydro char, is a valuable end-of-pipe product that could be used as solid fuel or sorbents for environmental decontamination [13, 14]. In subcritical water, the organic chlorine presence in PVC could be effectively converted to water-soluble inorganic chlorine, HCl, via elimination of HCl or nucleophilic substitution with water molecules as nucleophiles [15]. Previous studies have demonstrated that both hydrothermal treatment temperature and reaction time play a critical role in the dechlorination of PVC. High temperature or long treatment time would be required to achieve a high dechlorination efficiency, leading to high energy consumption for the treatment process [9, 16, 17]. To further improve the dechlorination efficiency of hydrothermal treatment, co-hydrothermal carbonization of biomass/municipal solid waste and PVC and additive-assisted hydrothermal treatment of PVC have received increasing attention. A large quantity of $^{\bullet}$OH radicals generated during biomass hydrothermal treatment could accelerate the dechlorination of PVC whilst the HCl generated could catalyze the hydrolysis and carbonization of biomass and reduce the ash content of hydrochar [18]. Different types of biowaste including bamboo, sawdust, straw, corncob and sewage sludge have been investigated and tested [19−23]. Additives including NaOH, KOH and Na_2CO_3 or ammonia could react with the formed HCl to promote the dechlorination efficiency [6,24-27].

The brief literature review has demonstrated the potential of the hydrothermal carbonization process for PVC waste management. According to ODI's report, the construction industry dominates the PVC market with about 50% of the PVC being used for manufacturing window profiles and pipes in the EU [3]. The notable feature of those PVC products is their composition containing a large number of additives including plasticisers, inorganic filler ($CaCO_3$) and stabiliser (TiO_2) which accounts for 20-60 wt% [28]. Although numerous studies have been carried out to investigate the hydrothermal treatment of PVC, PVC free from additives was used in most of the studies. The hydrothermal treatment of end-of-life PVC containing a large number of metal additives, the major component in waste PVC streams, has been rarely studied.

The impact of metal additives on the hydrothermal dichlorination of PVC and their migration pathways is crucial for the design of large-scale PVC treatment processes in the future. Moreover, the application of PVC-derived hydrochar is very limited as most of them have been tested as solid fuels and only a few works used them as solid sorbents for metal ions removal [20, 29]. Carbon-based sorbents have been considered as a promising candidate for CO_2 capture, thanks to their low-cost, fast adsorption kinetics and their novel thermal and chemical stability. Converting waste materials such as biomass and plastic to porous carbons is gaining attention owing to its wide availability and ability to simultaneously address waste recycling and carbon emission mitigation and a wide range of waste materials have been tested to prepare carbon materials for CO_2 capture. PVC-derived hydrochar, the major product from PVC recycling, represents a prospective easily available precursor for CO_2 sorbents preparation while its potential has not yet been evaluated. In this study, a typical PVC product containing a large quantity of additives, used PVC pipes, was selected as a single precursor to prepare hydrochar via the hydrothermal treatment method. The impact of hydrothermal treatment temperature and metal additives on the properties of hydrochar was investigated and evaluated. Moreover, the feasibility of using those hydrochars to prepare activated carbons for CO_2 adsorption was also explored.

2.0 Materials and methods

2.1 Preparation of activated carbon derived from waste PVC pipes

Waste PVC pipes were used as a single precursor to prepare activated carbons as shown in Figure 1. KOH used in this work was purchased from Fisher Scientific and used without any further treatment. In a typical procedure, 16 g dried PVC flakes mixed with 400 mL DI water was transferred to a hydrothermal reactor (Series 4530 2L Floor Stand Reactors), heated up to preset temperature (220, 240, 260 and 280 °C, respectively) and then kept for 1 h under continuous stirring. After being cooled down naturally to room temperature, the sample was washed with DI water and dried at 100 °C for further treatment.

Figure 1 Schematic diagram of PVC hydrochar derived activated carbons

Considering the low chlorine content present in hydrochar prepared at temperature higher than 260 °C (Figure 2), the PVC-derived hydrochar obtained at 260 °C was chosen as a precursor to prepare carbon material. 1 g hydrochar was subsequently impregnated in 10 mL potassium hydroxide (KOH) solution containing a certain amount of KOH (1 and 3 g, respectively) for 24 h before it was dried in an oven at 100 °C overnight. The dried sample was then transferred to a horizontal tube furnace and heated up from ambient to designed temperature 600/700/800 °C at a heating rate of 5 °C min^{-1} under 1 L min^{-1} nitrogen flow and kept at this temperature for 1 h. After the sample was cooled naturally to ambient temperature, the activated sample was collected and washed with DI water to remove the remaining activation agent until the filtrate became neutral. Finally, all the carbons prepared using PVC-derived hydrochar labelled as HPVC-a-b, where a and b respectively represent the activation temperature and the mass ratio between KOH and PVC, were obtained after being dried in the oven at 100 °C overnight.

2.2 Characterization

The elemental compositions of the PVC-derived hydrochar and selected activated carbons were obtained by using X-ray fluorescence (XRF) spectroscopy (Bruker S8 Tiger). Proximate analysis of hydrothermally treated PVC samples was carried out using a thermogravimetric analyser ((TGA-Q500, TA instruments: weighing accuracy of +/- 0.1%, sensitivity < 0.1 μg and isothermal temperature accuracy of +/- 1 °C)). In a typical procedure, the sample was first heated up to 105 °C in a flow of N_2 for 30 min to determine the moisture content and then the devolatilization step was conducted by heating the sample to 900 °C at a heating rate of 20 °C min^{-1}. After 15 min, the sample was cooled down to 800 °C to initiate the combustion process whilst the gas was switched to air. The dechlorination efficiency was estimated using the following equation:

$$Dechlorination\ effciency = 100 \times \frac{Cl_{PVC} - Cl_{product,T} \times Y_T}{Cl_{PVC}}$$

Where Cl_{PVC} and $Cl_{product,\ T}$ represent the concentration of chlorine in the original PVC and the hydrochar obtained at the hydrothermal temperature of T, respectively. Y_T is the yield of hydrochar at the hydrothermal temperature of T. The removal rate of calcium was calculated using the same equation. TGA and XRF test of a selected sample was repeated 3 times, which only gave a difference of <1%, indicating that the results are reliable. The nitrogen adsorption isotherms of the prepared carbon samples at −196 °C were obtained by using Micromeritics ASAP 2420 analyser. All samples were degassed at 150 °C for 16 h before testing. The non-local density functional theory (NLDFT) model was used to calculate the pore volume and pore size distribution of all samples by using the combination of CO_2 adsorption isotherm with N_2 adsorption isotherm obtained at −196 and 0 °C, respectively. The morphological properties of selected hydrochar-derived carbon samples were characterized by using a field-emission scanning electron microscope (FEI-SEM).

2.3 CO_2 adsorption performance

The CO_2 adsorption performance of the PVC-derived carbons was evaluated by their CO_2 adsorption isotherms measured on Micromeritics ASAP 2420 at 0 and 25 °C. Nitrogen adsorption isotherm of all carbon samples at 25 °C was also obtained to calculate their CO_2/N_2 selectivity. The isosteric heat of CO_2 adsorption (Q_{st}) for all samples was evaluated by using the Clausius-Clapeyron equation. Dual-site Langmuir (DSL) model was used to fit the CO_2 adsorption isotherms to obtain all parameters required for the Clausius-Clapeyron equation. The DSL model can be explained as follows:

$$q = \frac{q_A \times b_A \times p}{1 + b_A \times p} + \frac{q_B \times b_B \times p}{1 + b_B \times p}$$

Where q, q_A and q_B represent the adsorption capacity and mono-layer CO_2 capacity of site A and B at equilibrium pressure of p, respectively. b_A and b_B are the adsorption equilibrium constants for site A and B, respectively.

3.0 Results and discussion

3.1 hydrothermal carbonization of PVC waste

Hydrothermal treatment of PVC pipe waste was carried out at temperature ranging between 220 and 280 °C for 1 h and the results are shown in Figure 2. Figure 2a shows the yield of solid residue as a function of hydrothermal treatment temperatures from 220 to 280 °C. Clearly, the hydrothermal treatment of PVC could be divided into two stages. At temperatures between 220 and 260 °C, the yield of solid residue decreased continuously from 80 to 41 wt% with increasing temperature, which is mainly attributable to the degradation of PVC by dechlorination and formation of double bonds in polyene sequences ($-(CH=CH)_n-$) [15]. When the temperature further increased to 280 °C, the initial decomposition of polyene followed by aromatization and polymerization of the decomposition products to hydrochar occured and the yield of solid residue barely changed. According to the proximate analysis shown in Figure 2a, the fixed carbon content of hydrochar continuously increased with hydrothermal treatment temperature from 11.49 wt% of raw PVC to 30.32 wt% when the hydrothermal treatment temperature increased to 280 °C. Moreover, the ash content of the original PVC waste was about 20 wt%, consisting of mainly calcium carbonate, which is vastly different from the pure PVC polymer with a trace amount of ash used in most previous studies. Hydrothermal treatment of PVC led to a sharp decrease in ash content from 20 wt% to less than 6 wt% in solid residue, accounting for over 90% removal efficiency, at temperatures over 240 °C. This suggests that most of the metal additives in PVC have been removed and transferred to an aqueous solution during the hydrothermal treatment process and the solid product with low ash content could be potentially used as a solid fuel or carbon precursor to manufacture porous carbon materials.

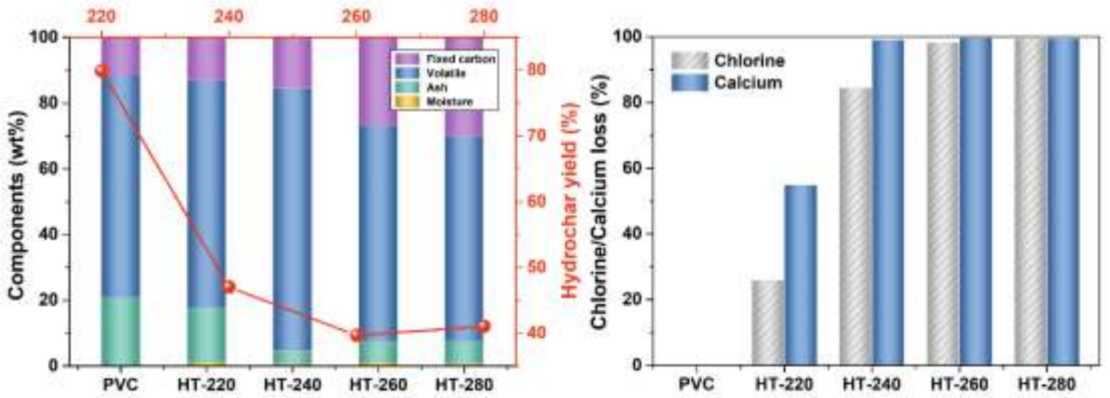

Figure 2 Hydrothermal treatment of PVC: (a) proximate analysis of original PVC and PVC-derived hydrochar and hydrochar yield; (b) dechlorination efficiency and calcium removal of PVC as a function of hydrothermal temperature.

Dechlorination of PVC is the key step before any practical application. Figure 2b shows the behavior of chlorine in hydrochar represented by removal rate as a function of hydrothermal treatment temperature. Hydrothermal temperature plays a critical role in chlorine removal. At the hydrothermal temperature of 220 °C, the dechlorination efficiency was about 26.01%. It was significantly increased to 98.36% when the hydrothermal temperature rose to 260 °C at a reaction time of only 1 h. At the hydrothermal temperature of 280 °C, the chlorine in PVC was almost completely removed with dechlorination efficiency reaching 99.39%. Table 1 summarizes the dechlorination efficiency reported in previous studies. It can be seen that the dechlorination efficiency obtained in this study was much higher than the dechlorination efficiency of pure PVC and comparable to or even higher than biomasses or additives-assisted dechlorination of PVC under similar conditions and reaction time. This suggests that the dechlorination reactions in used PVC pipe were accelerated.

Table 1 The dechlorination efficiency of PVC reported in previous studies

Sample	Particle size	Ash content wt%	Temperature (°C)	Additives	Time (h)	Dechlorination ratio	Reference
Used PVC pipe	strips 20 ×2 ×2 mm	20	260	--	1	98.36	This work
		20	280	--	1	99.39	
PVC	< 0.15 mm	0.4	280	--	0.5	82.51	[17]

PVC + lignin	< 0.25 mm	--	210		2	89.50	[18]
PVC + pine sawdust	powder	0	260	--	2	84.15	[19]
PVC + sewage sludge	--	0.03	230	--	1	81.35	[20]
PVC + lignocellulose biomass	--	0.24	240	--	1.5	92.47	[22]
PVC + bamboo	powder	0	260	--	1	91.79	[23]
PVC + coal gangue	3–5 mm	0	220	--	1	96.30	[30]
PVC + pine wood	< 0.074 mm	0.3	280	--	0.5	93.90	[31]
PVC + corncob	< 0.074 mm	0	260	--	0.5-1.5	89.29	[32]
PVC	< 0.25 mm	< 0.6	260	Citric acid	15	98.00	[9]
PVC + corncob	powder	0	260	Citric acid	1	93.63	[21]
PVC electric wires	<3 mm	--	250	K_2CO_3	1	14.60	[24]
			250	K_2CO_3	4	99.10	
PVC			260	NaOH	0.5	86.00	[33]
PVC	powder	--	250	NH_3	1	95.00	[34]
PVC	0.10–0.20 mm	0	220	$Cu(NO_3)_2$	1	86.50	[35]

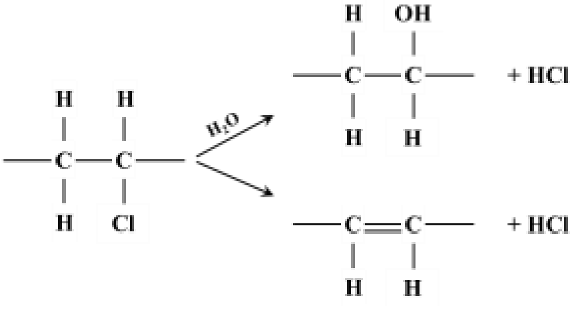

(1)

$$CaCO_3 + HCl \rightleftharpoons CaCl_2 + H_2O \qquad (2)$$

According to previous studies, the chlorine in the polymer backbone could be removed in subcritical water via two main pathways (reaction 1): elimination and substitution. As shown in the following reactions (equation 1), the chlorine in PVC was removed in the form of HCl from both pathways, which requires high hydrothermal temperature and long reaction time to achieve high dichlorination efficiency.. The high dechlorination efficiency of PVC at the relatively mild condition and short treatment time in this research is attributable to the in-situ calcium carbonate. The role of calcium carbonate is similar to the additives such as K_2CO_3, ammonia and NaOH, which could potentially neutralize the formed HCl from different reaction pathways as shown in reaction 1 and 2 and therefore accelerate the dechlorination process. As shown in Figure 2c, an almost linear relationship between calcium removal efficiency and dechlorination efficiency as a function of temperature was observed. Moreover, Moreover, the well-distributed $CaCO_3$ micro/nano particles acted as an in-situ neutralization agent that could react with released HCl instantly within the PVC matrix. In previous studies, PVC in the form of fine powder or small particles (< 5 mm) was used in most of the previous studies (Table 1) to reduce the diffusion resistance of formed HCl from inside the PVC which is one of the rate-determining steps during hydrothermal dichlorination of PVC [34]. The in-situ $CaCO_3$ could minimize the diffusion resistance of HCl while the consumption of $CaCO_3$ could create extra channels for $CaCl_2$/HCl molecules, which lowered the impact of particle size on the dechlorination process. Even higher dechlorination rate could be achieved within 1 h by using large PVC strips (L×W×D: 20 mm×2 mm×2 mm) than most powdered PVC reported previously. This is crucial for the design of a cost-effective recycling process of end-life PVC pipes or window profiles as the demand for pulverization, an energy-intensive process, can be largely reduced. $CaCl_2$, a major by-product of dichlorination, has been reported as an effective catalyst for hydrothermal treatment of biowastes such as improving the dewaterability of activated sludge or liquid yield of oily scum, suggesting that PVC can be used as a promoter for hydrothermal treatment of other biowastes. The results suggest that hydrothermal treatment can be a potential technology to recycle waste PVC containing a large quantity of additives content for the production of high-quality hydrochar..

3.2 Characterization of PVC hydrochar derived carbons

Converting waste plastic, the carbon-rich precursor, to porous carbon materials has been considered as a potential pathway to deal with those non-degradable waste. By removal of chlorine via hydrothermal treatment, the chlorine-free hydrochar can be potentially used as a carbon precursor to prepare microporous carbon materials for many applications including CO_2 adsorption, which has not yet been studied. Therefore, to investigate the feasibility of PVC hydrochar-derived carbons for CO_2 adsorption, PVC-derived hydrochar prepared at 260 °C was selected as a single carbon precursor to produce porous carbon materials via a facile one-step chemical activation method using KOH as activating agent. The nitrogen adsorption isotherms and corresponding pore size distributions (PSDs) of HPVC carbons in the activation temperature range between 600−800 °C and KOH/PVC mass ratio of 1 and 3 are shown in Figure 3. The sharp N_2 adsorption capacity at extremely low relative pressure followed by a horizontal plateau at high relative pressure indicates the microporous nature of HPVC carbons. For carbons prepared at high activation temperature of 800 °C or KOH/PVC mass ratio of 3, a small hysteresis loop at P/P_0 >0.50 corresponds to the presence of mesoporous structure containing slit-like mesopores. It can be seen from Figure 3c, d that the carbon samples prepared under different conditions were comprised mostly of micropores while the significance of micropores with different pore width varied with the preparation conditions. The pores in the carbon sample prepared at an activation temperature of 600 °C and KOH/PVC mass ratio of 1 were purely ultra-micropores with pore size smaller than 0.50 nm. As the activation temperature and KOH/PVC mass ratio increased, the micropores centered at 0.55 and 1.20 nm started to emerge and ultra-micropores centred at 0.55 nm became dominant. This highlights the pore-widening effect induced by high activation temperature or excessive KOH. The ultra-microporous nature offers the potential capability of HPVC carbons as CO_2 adsorbents.

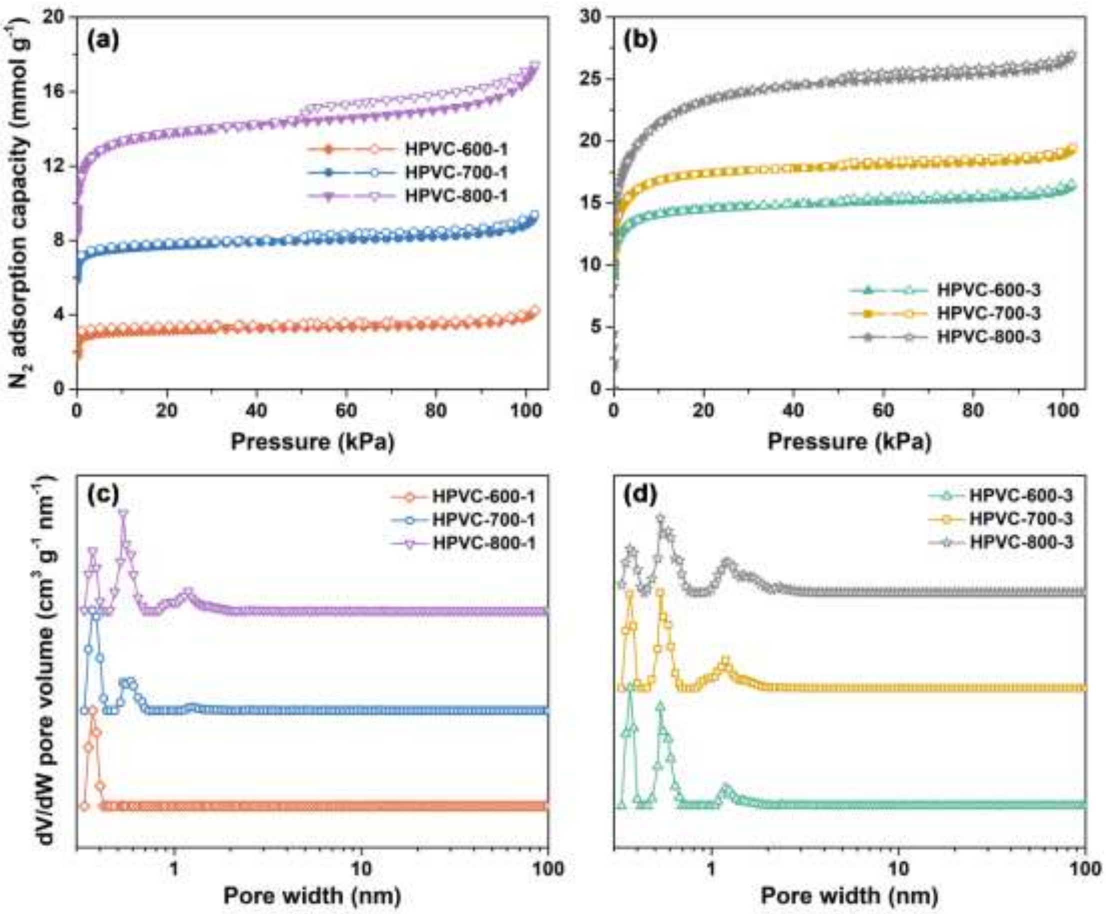

Figure 3 Nitrogen isotherms and pore size distributions (PSDs) of HPVC carbons: (a and b) nitrogen adsorption isotherms; (c and d) PSDs.

The textural properties of PVC hydrochar-derived activated carbons are shown in Table 2. It can be seen that both BET surface area and total pore volume sharply increased with activation temperature and KOH/PVC mass ratio from only 285 m^2 g^{-1} and 0.14 cm^3 g^{-1} for HPVC-600-1 to 1927 m^2 g^{-1} and 0.85 cm^3 g^{-1} for HPVC-800-3, respectively. This is attributed to the enhanced KOH activation reactions in the presence of excessive KOH or higher activation temperature. As shown in Figure 3c-d, the HPVC carbons mainly consist of ultra-micropores with pore size <0.7 nm, which is expected to be a preferable place for CO_2 adsorption. At the KOH/PVC mass ratio of 1, the ultra-micropore volume increased from 0.11 to 0.26 cm^3 g^{-1} as the activation temperature increased to 800 °C. When the KOH/PVC mass ratio increased to 3, all samples showed a similar ultra-micropore volume of 0.29−0.33 cm^3 g^{-1} and the increase of activation temperature even led to a slight decrease in ultra-micropore volume.

Moreover, the ratio of the ultra-micropore volume to the micropore volume ($V_{micro<0.7nm}/V_{micro}$) and total pore volume ($V_{micro<0.7nm}/V_{micro}$) calculated based on the data shown in Table 2 showed that the relative fraction of $V_{micro<0.7nm}/V_{micro}$ and $V_{micro<0.7nm}/V_{micro}$ decreased with increasing activation temperature or KOH/PVC mass ratio. This suggests that pore formation predominated at mild activation temperature and low KOH/PVC mass ratio whereas pore widening played the leading role when higher activation temperature or excessive KOH were used.

Table 2 Textural properties of porous matrixes and their derived salt composites.

Sample	S_{BET} (m^2/g)	V_{total} (cm^3/g)	V_{micro} (cm^3/g)	$V_{micro<0.7nm}$ (cm^3/g)
HPVC-600-1	285	0.14	0.11	0.11
HPVC-700-1	697	0.30	0.25	0.22
HPVC-800-1	1206	0.55	0.44	0.26
HPVC-600-3	1283	0.52	0.47	0.33
HPVC-700-3	1519	0.61	0.56	0.29
HPVC-800-3	1927	0.85	0.71	0.30

The morphologies of PVC hydrochar-derived carbons examined with scanning electron microscopy (SEM) are shown in Figure 3. Clearly, all samples are granular with a relatively wide particle size distribution whilst the microporous structure of HPVC carbons varied significantly with the KOH/PVC mass ratio and activation temperature. Sample HPVC-700-1 exhibited a less porous structure and denser porous network compared to the sample prepared at a higher KOH/PVC mass ratio of 3. The excessive KOH enhanced the formation of more pores and interconnected macroporous structure via multiple reactions between KOH and carbon during the activation process. For instance, HPVC-600-3 demonstrated a highly macroporous structure with high pore interconnectivity. The macroporous structure of PVC hydrochar-derived carbon was further developed as the activation temperature increased to 700 °C. It can be found from the high-resolution images (Figure 4f, i) that HPVC-700-3 is much more porous than HPVC-600-3, which is attributable to the enhanced activation efficacy led by higher temperature.

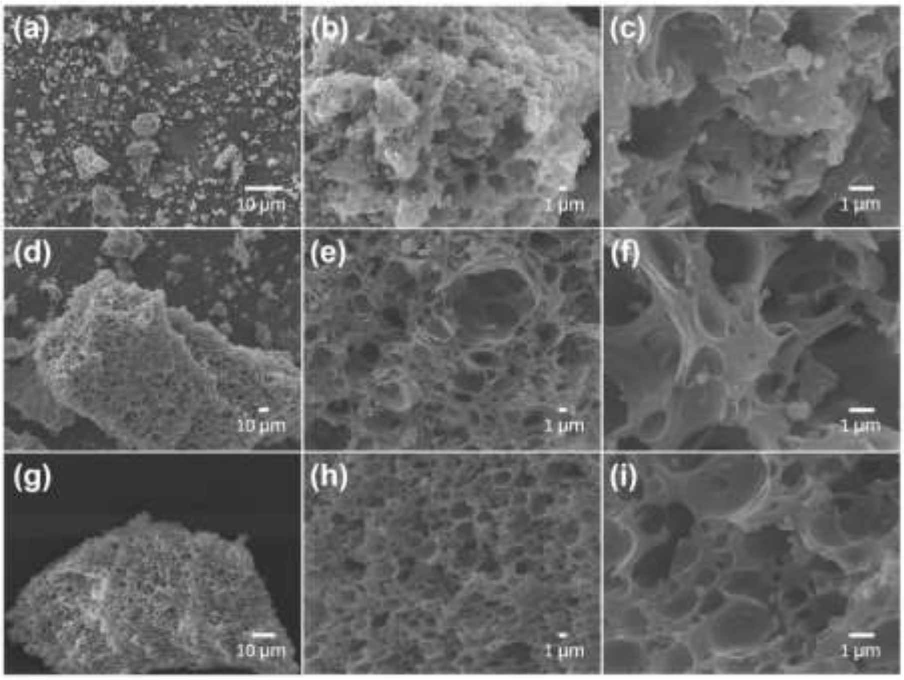

Figure 4 SEM images of HPVC carbons: (a-c) HPVC-700-1; (d-f) HPVC-600-3; (g-j) HPVC-700-3.

3.3 CO_2 adsorption performance of HPVC carbons

The CO_2 adsorption isotherms at 0 °C and 25 °C, up to 100 kPa pressure are shown in Figure 5. The results demonstrated the good CO_2 adsorption performance achieved by HPVC carbons at different temperatures. At 0 °C and 100 kPa, HPVC-600-3 exhibited the highest CO_2 adsorption capacity of 6.21 mmol/g among all samples. Reducing KOH/PVC mass ratio or increasing activation temperature both led to a decrease in CO_2 adsorption capacity. According to Table 1, the CO_2 adsorption capacity of different carbons generally follows the trend of their ultra-micropore volume, which suggests that the high CO_2 adsorption capacity of HPVC-600-3 is driven by its high ultra-micropore volume ($V_{micro<0.7\ nm}$). When the adsorption temperature was increased to 25 °C, a similar trend was observed with HPVC-600-3 achieving the highest adsorption capacity of 4.05 mmol/g. However, being different from 0 °C, the adsorption capacity of HPVC-700-1 was slightly higher than that of HPVC-800-3 with much higher ultra-micropore volume than HPVC-700-1, indicating that smaller ultra-micropores play a critical role in CO_2 adsorption at higher temperatures. A more pronounced discrepancy is observed at the low CO_2 partial pressure region. For instance, at CO_2 partial pressure of 15 kPa, HPVC-600-3 and HPVC-700-1 exhibited much higher CO_2 adsorption capacities of 2.64 and 2.50 mmol g^{-1} at 0 °C, respectively. When the adsorption temperature was increased to 25 °C, HPVC-700-1 achieved the highest adsorption of 1.60 mmol g^{-1} among all samples. This suggests that the CO_2 adsorption performance of HPVC carbons was determined by ultra-micropores with a specific pore size, which varies with the adsorption temperature and CO_2 partial pressure. Previous studies have demonstrated that the critical pore size for CO_2 adsorption decreased with increasing adsorption temperature or decreasing CO_2 partial pressure. More specifically, pores smaller than 0.6 nm are preferred for CO_2 adsorption at 100 kPa and 25 °C while it reduced to 0.5 nm when the CO_2 partial pressure dropped to 15 kPa. In this study, the correlation between the volume of pores smaller than a specific pore size and CO_2 adsorption capacity at different conditions was studied (Figure S1). It can be observed that the CO_2 adsorption capacity of HPVC carbons at 15 and 100 kPa gave the best correlation with the volume of pores smaller than 0.44 nm and 0.60 nm at 25 °C, respectively. When the adsorption temperature decreased to 0 °C, pores smaller than 0.60 nm and 0.80 nm are preferable for CO_2 adsorption at 15 and 100 kPa, respectively. Those results agree well with the findings reported in previous studies that ultramicroscope plays a critical role in capturing CO_2.

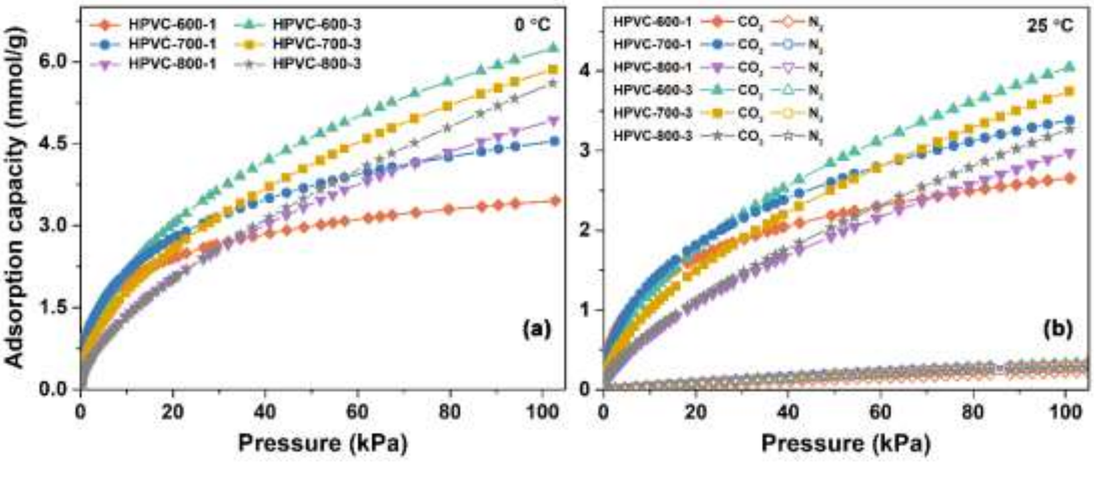

Figure 5 CO_2 adsorption isotherm of the HPVC carbons at 0 °C and 25 °C.

The preparation of carbon-based CO_2 sorbents from using waste materials such as biomass or plastic waste has increasingly received attention as a potential approach for waste management. Table 3 summarizes the CO_2 adsorption capacity of plastic or biomass-derived carbon materials, prepared by chemical activation using KOH as activating agent, reported in previous studies. It can be found that well-developed microporosity and surface chemistry make HPVC carbons prepared in this paper one of the best-performing carbon-based sorbents for CO_2 adsorption especially at low CO_2 pressure region. At low CO_2 partial pressure of 15 kPa, the CO_2 adsorption capacity of HPVC carbons could reach 1.50-1.60 mmol g^{-1}, which outperforms the majority of plastic or biomass-derived carbons. This highlights that PVC can be a potential precursor to prepare excellent sorbents for CO_2 mitigation.

As shown in Table 3, PVC has been used as a single precursor to prepare carbon-based CO_2 sorbents via oxidation-activation protocol in previous studies. It can be seen that the CO_2 adsorption capacity of carbons prepared by using pure PVC is much higher than carbons prepared using PVC with a large quantity of metal additives, which is attributable to a much higher volume of fine micropores (< 0.5 nm) of pure PVC derived carbons created by KOH activation. However, the CO_2 adsorption capacity at low partial pressure regions cannot be solely rationalized by the pore size effect. For instance, waste PVC pipe-derived carbons prepared via an oxidation-KOH activation process in our previous study had a high volume of pores smaller than 0.44 nm, 0.153 cm^3 g^{-1} (P_71), which was higher than the samples prepared in this paper, while the adsorption capacity of P_71, 1.16 mmol g^{-1}at 25 °C and 15 kPa, was much lower than HPVC-700-1 of 1.60 mmol g^{-1} [41]. It is believed that surface chemistry might also play a critical role in CO_2 adsorption at low CO_2 partial pressure. Given the fact that PVC is a nitrogen-free precursor, the intercalated potassium formed during the KOH activation process, which has been reported in previous studies [44, 51], could favor CO_2 adsorption at low partial pressure. According to the XRF results, the potassium content of HPVC-700-1was 6.89 wt% which was much higher than P_71 of 3.64 wt%. The intercalated potassium on the carbon surface acted like the extra framework ions in MOFs and zeolites, which could effectively improve the surface affinity of carbon to

CO_2 and provide extra CO_2 adsorption sites. Similarly, Wang et al. [40] found that the residue potassium in PVC-derived carbon spheres could significantly improve the CO_2 adsorption capacity and the removal of potassium led to a sharp decrease of 75% in CO_2 adsorption capacity. The unique combination of fine micropores and surface chemistry makes PVC hydrochar-derived carbons an excellent sorbent for CO_2 adsorption.

Table 3 A summary of CO_2 adsorption performance of waste-derived carbon materials.

Precursors	Activation strategy	CO_2 adsorption capacity at 100 kPa (mmol g^{-1})				References
		0 °C		25 °C		
		15 kPa	100 kPa	15 kPa	100 kPa	
HPVC-6003	**KOH**	**2.64**	**6.21**	**1.51**	**4.05**	**This work**
HPVC-7001	**KOH**	**2.50**	**4.52**	**1.60**	**3.40**	
Waste CDs and DVDs	KOH	1.80^a	5.80^a	0.85^a	3.30^a	[36]
Cigarette filter	KOH	1.70^a	6.06	1.00	3.55^a	[37]
Packaging waste	KOH	1.75	5.30	0.80^a	4.20	[38]
PET plastic bottle (N-dopped)	KOH	2.60^a	6.23	1.60^a	4.58	[39]
PVC-Derived Carbon Sphere	KOH	4.40^a	8.93	2.45^a	5.47	[40]
Used PVC pipe	KOH	1.76	6.90	0.85	3.90	[41]
Carrot peels	KOH	2.00^a	5.64	1.13^a	4.18	[42]
Coffee ground	KOH	2.20^a	7.55	1.40^a	4.42	[43]
Rice husk	KOH	2.96	5.91	2.00	4.75	[44]
Bamboo	KOH	2.29^a	7.00	1.36	4.50^a	[45]
Date sheet	KOH	1.80^a	6.40	0.92^a	4.36	[46]
Glucose	KOH	2.45	5.91	1.44	4.30	[47]
Empty fruit bunch	KOH	1.84^a	5.23	1.32^a	3.71	[48]
Lotus stalk	KOH	1.96	5.11	1.21	3.68	[49]
Water caltrop shell	KOH	2.00^a	5.86	1.25^a	4.22	[50]

Note: a-the adsorption capacity was estimated based on the adsorption isotherms provided.

The high surface affinity of HPVC carbons could also be indicated by the isosteric heat of CO_2 adsorption (Q_{st}) calculated by using the Clausius-Clapeyron equation. All the parameters were obtained by fitting the CO_2 adsorption isotherms at 0 and 25 °C by using dual-site Langmuir (DSL) model. It can be seen from Figure 6 that the Q_{st} for all samples continuously decreases with increasing CO_2 adsorption capacity and remains stable at CO_2 adsorption capacity over 2 mmol g^{-1}. This suggests CO_2 was preferably adsorbed on strong surface adsorption sites followed by adsorption on weaker surface adsorption sites. At zero CO_2 coverage, high Q_{st} ranging from 35.74 to 39.18 kJ mol^{-1} was achieved by HPVC carbons, which was much higher than dopant-free carbons or some nitrogen-doped carbons [52−54]. This clearly shows that the combination of surface heterogeneity originating from potassium and ultra-micropores created strong surface adsorption sites which is more beneficial to CO_2 adsorption at low CO_2 partial pressure. This can be further verified when the Q_{st} of HPVC-600-1 was compared to other HPVC carbons. As shown in Figure 5, HPVC-600-1 with pure fine micropores ($d<0.50$ nm) exhibited much higher Q_{st} than other samples especially at high CO_2 coverage.

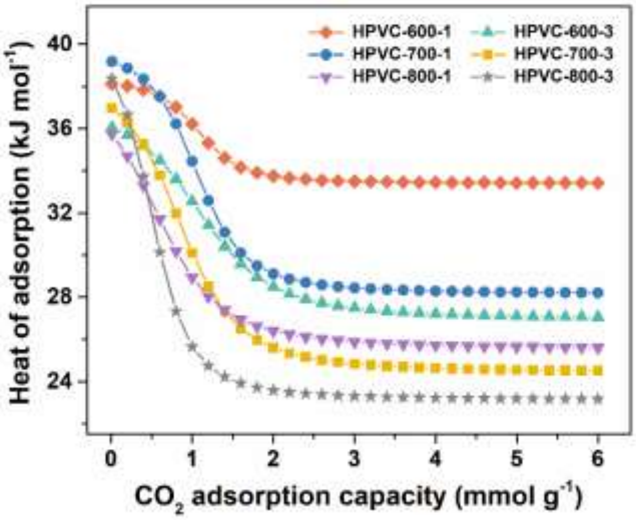

Figure 6 Isosteric heat of CO_2 adsorption on carbon foams calculated from the adsorption isotherms at 0 and 25 °C.

3.4 CO_2/N_2 Selectivity

In addition to high adsorption capacity, an ideal CO_2 sorbent should also be able to effectively separate CO_2 from flue gas mainly containing CO_2 and N_2. The CO_2/N_2 selectivity of HPVC carbons was estimated by using the ideal adsorption solution theory (IAST) model. Both CO_2 and N_2 adsorption isotherms obtained at 25 °C were fitted with a DSL model to get selectivity parameters according to IAST. Figure 7 exhibits the calculated CO_2/N_2 selectivity of HPVC carbons in the different gas mixture as a function of bulk pressure. It can be found that the CO_2/N_2 selectivity decreased continuously with increasing bulk pressure from 5 kPa to 100 kPa and CO_2 partial pressure in the CO_2/N_2 gas mixture. This can be explained by the higher growth rate in N_2 adsorption capacity compared to CO_2 with increasing pressure. On the other hand, this also suggests that the adsorption rate of CO_2 at the initial adsorption stage was much higher than N_2, which is attributable to the larger quadruple of CO_2 and the high surface affinity created by potassium. Despite the microporous nature of all HPVC carbons, a noticeable variation in CO_2/N_2 selectivity was observed among different samples. The selectivity generally decreased with increasing activation temperature and KOH/PVC mass ratio. As shown in Figure 6d, the CO_2/N_2 selectivity over the HPVC carbons is in agreement with the relative fraction of volume of pores smaller than 0.5 nm to total pore volume. Considering the smaller kinetic diameter of the CO_2 molecule than the N_2 molecule (0.334 vs 0.364 nm), the enhanced activation efficacy by high activation temperature and KOH/PVC mass ratio created a significant amount of large micropores (>0.50 nm) leading to the increase of N_2 adsorption capacity at the same CO_2 partial pressure. Among all samples, HPVC-600-1 with an almost pure fine micropore ($d < 0.50$ nm) exhibited the highest CO_2/N_2 selectivity under different conditions. For instance, at a realistic gas pressure of 100 kPa, the CO_2/N_2 selectivity of HPVC-600-1 could reach 83.86 for a 5:95 CO_2/N_2 mixture (flue gas from the natural gas power plant) and 42.15 for a 15:85 CO_2/N_2 mixture (flue gas from the coal-fired power plant), which is higher than the majority carbons reported in previous studies [55−58].

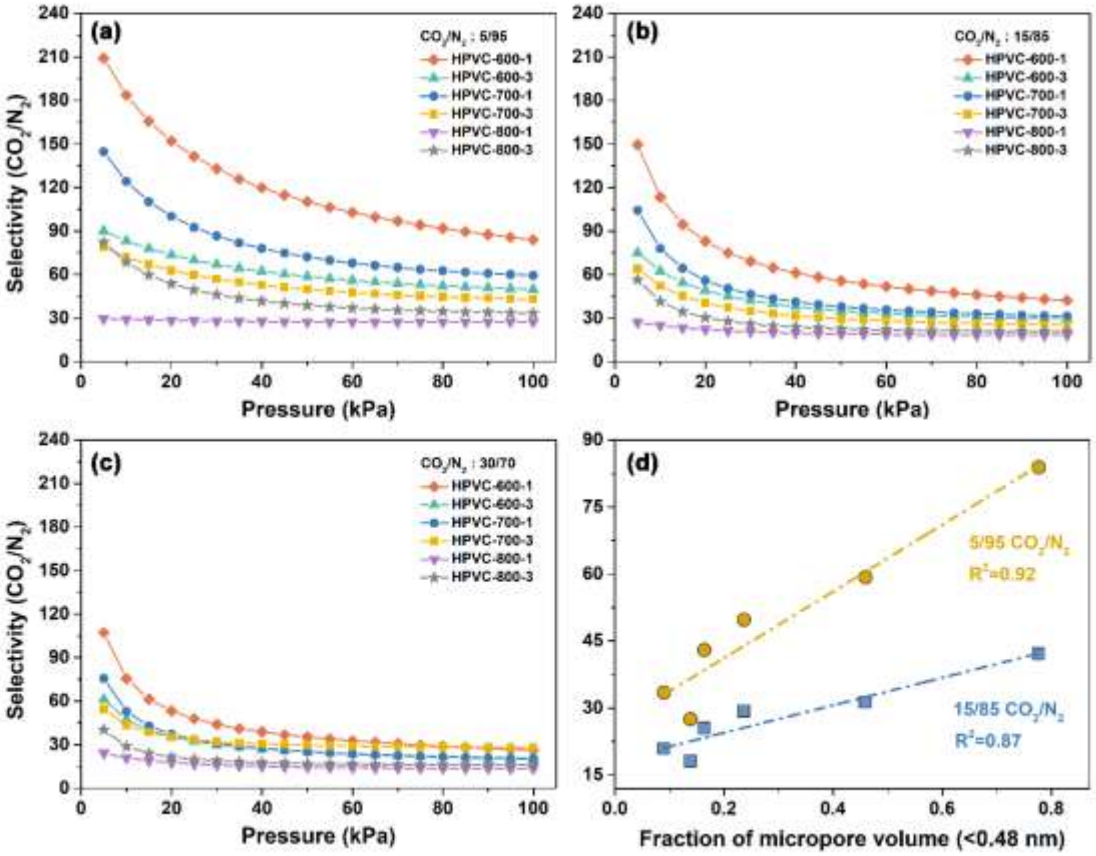

Figure 7 The CO_2/N_2 selectivity of HPVC carbons in different gas mixture:(a) 5% CO_2 in N_2; (b) 15% CO_2 in N_2; (c) 30% CO_2 in N_2; (d) relationship between ultra-micropore volume and CO_2/N_2 selectivity of HPVC carbons.

4.0 Conclusions

In summary, this work demonstrated a potential strategy to utilize hard-to-handle waste PVC plastic, the top 3 plastics in waste streams, for the preparation of chlorine-free carbon-based efficient sorbents for CO_2 mitigation via a hydrothermal dichlorination-chemical activation protocol. Being different from most previous studies that use pure PVC plastic as a precursor, waste PVC with a large quantity of metal additives, a major component in waste PVC plastic, was hydrothermally treated and the impact of metal additives on the dechlorination process was also investigated. The results showed that a high dechlorination rate of 98.40% and 99.39% was obtained at a temperature of 260 and 280 °C and a reaction time of 1 h, respectively, which was higher than the dechlorination efficiency of pure PVC and many biomasses or additives-assisted dechlorination of PVC under similar conditions. The large quantity of well-distributed calcium carbonate in the PVC matrix could effectively accelerate the dechlorination reactions by in-situ neutralization of released HCl within the PVC matrix. The consumption of calcium carbonate could create extra channels for the diffusion of $CaCl_2$/HCl from inside PVC, which can potentially lower the impact of particle size and reduce the demand for pulverization.

Using chlorine-free PVC hydrochar as a single precursor, microporous carbons were successfully synthesized via a facile chemical activation process and evaluated as sorbents for CO_2 adsorption. Tested at an adsorption temperature of 25 °C, a high CO_2 adsorption capacity of 1.60 mmol/g at 15 kPa CO_2 and 4.05 mmol/g at 100 kPa as we as high CO_2/N_2 of 42 at 15 kPa CO_2 was obtained by those carbons, which is among the best-performing plastic or biomass waste-derived carbons. Advanced characterization demonstrated that the development of large ultra-micropore volume and surface chemistry with high CO_2 affinity granted the highly selective CO_2 capture in those hydrochar-derived carbons. The data reported in this work has practical implications for the safe and sustainable recycling of waste PVC plastics and the development and design of PVC-derived sorbents for CO_2 emission mitigation.

Acknowledge

This work was supported by the China Postdoctoral International Postdoctoral Exchange Fellowship Program and the UK Carbon Capture and Storage Research Centre (EP/P026214/1). The UKCCSRC is supported by the EPSRC as part of the UKRI Energy Programme. The authors also thank Ms. Teresa Needham for assisting in the measurements of XRF.

References

[1] Miliute-Plepiene J, Fråne A, Almasi A M. Overview of polyvinyl chloride (PVC) waste management practices in the Nordic countries. Chem Eng Technol 2021; 4:100246.

[2] Oster K, Tedstone A, Greer A J, Budgen N, Garforth A, Hardacre C. Dehydrochlorination of PVC in multi-layered blisterpacks using ionic liquids. Green Chem 2020; 22(15):5132-5142.

[3] Scott A, Pickard S, Sharp S, Becqué R. Phasing out plastics. ODI Report 2020.

[4] Plastic Europe, EPRO. Plastics-The Facts 2021, https://plasticseurope.org/knowledge-hub/plastics-the-facts-2021/; 2021[accessed 13 March 2022].

[5] Buekens A, Cen K. Waste incineration, PVC, and dioxins. J Mater Cycles Waste Manag 2011; 13(3):190-197.

[6] Yoshioka T, Kameda T, Imai S, Noritsune M, Okuwaki A. Dechlorination of poly (vinylidene chloride) in NaOH/ethylene glycol as a function of NaOH concentration, temperature, and solvent. Polym degrad stab 2008; 93(10):1979-1984.

[7] Chang Y, Pang Y, Dang Q, Kumar A, Zhang G, Chang Z, et al. Converting polyvinyl chloride plastic wastes to carbonaceous materials via room-temperature dehalogenation for high-performance supercapacitor. ACS Appl Energy Mater 2018; 1(10):5685-5693.

[8] Lu J, Borjigin S, Kumagai S, Kameda T, Saito Y, Yoshioka T. Practical dechlorination of polyvinyl chloride wastes in NaOH/ethylene glycol using an up-scale ball mill reactor and validation by discrete element method simulations. Waste Manag 2019, 99: 31-41.

[9] Poerschmann J, Weiner B, Woszidlo S, Koehler R, Kopinke F D. Hydrothermal carbonization of poly (vinyl chloride). Chemosphere 2015; 119:682-689.

[10] Zhang G, Wang L, Hao Y, Jin X, Xu Y, Kuang Y, et al. Unconventional carbon: alkaline dehalogenation of polymers yields N-doped carbon electrode for high-performance capacitive energy storage. Adv Funct Mater 2016; 26(19):3340-3348.

[11] Vidal R, Alberola-Borràs J A, Habisreutinger S N, Gimeno-Molina J L, Moore D T, Schloemer T H, et al. Assessing health and environmental impacts of solvents for producing perovskite solar cells. Nat Sustain 2021, 4(3): 277-285.

[12] Chang S H. Utilization of green organic solvents in solvent extraction and liquid membrane for sustainable wastewater treatment and resource recovery—a review. Environ Sci Pollut Res 2020, *27*(26): 32371-32388.

[13] Li H Z, Zhang Y N, Guo J Z, Lv J Q, Huan W W, Li B. Preparation of hydrochar

with high adsorption performance for methylene blue by co-hydrothermal carbonization of polyvinyl chloride and bamboo. Bioresour Technol 2021; 337:125442.

[14] Ning X, Teng H, Wang G, Zhang J, Zhang N, Huang C, et al. Physiochemical, structural and combustion properties of hydrochar obtained by hydrothermal carbonization of waste polyvinyl chloride. Fuel 2020; 270:117526.

[15] Takeshita Y, Kato K, Takahashi K, Sato Y, Nishi S. Basic study on treatment of waste polyvinyl chloride plastics by hydrothermal decomposition in subcritical and supercritical regions. J Supercrit Fluids 2004; 31(2):185-193.

[16] Soler A, Conesa J A, Ortuño N. Application of subcritical water to dechlorinate polyvinyl chloride electric wires. Energies 2018; 11(10):2612.

[17] Yang M, Zhao P, Cui X, Geng F, Guo Q. Kinetics study on hydrothermal dechlorination of poly (vinyl chloride) by in-situ sampling. Environ Technol Innov 2021; 23:101703.

[18] Shen Y, Yu S, Ge S, Chen X, Ge X, Chen M. Hydrothermal carbonization of medical wastes and lignocellulosic biomass for solid fuel production from lab-scale to pilot-scale. Energy 2017; 118:312-323.

[19] Huang N, Zhao P, Ghosh S, Fedyukhin A. Co-hydrothermal carbonization of polyvinyl chloride and moist biomass to remove chlorine and inorganics for clean fuel production. Appl Energy 2019; 240:882-892.

[20] Lu X, Ma X, Qin Z, Chen X, Chen L, Tian Y. Co-hydrothermal carbonization of sewage sludge and polyvinyl chloride: Hydrochar properties and fate of chlorine and heavy metals. J Environ Chem Eng 2021; 9(5):106143.

[21] Lu X, Ma X, Chen X, Yao Z, Zhang C. Co-hydrothermal carbonization of polyvinyl chloride and corncob for clean solid fuel production. Bioresour Technol 2020; 301:122763.

[22] Xue Y, Bai L, Chi M, Xu X, Chen Z, Yu K, et al. Co-hydrothermal carbonization of pretreatment lignocellulose biomass and polyvinyl chloride for clean solid fuel production: Hydrochar properties and its formation mechanism. J Environ Chem

Eng 2022, 10(1):106975.

[23] Yao Z, Ma X. Characteristics of co-hydrothermal carbonization on polyvinyl chloride wastes with bamboo. Bioresour Technol 2018; 247:302-309.

[24] Gandon-Ros G, Soler A, Aracil I, Gómez-Rico M F. Dechlorination of polyvinyl chloride electric wires by hydrothermal treatment using K_2CO_3 in subcritical water. J Waste Manag 2020; 102:204-211.

[25] Li T, Zhao P, Lei M, Li Z. Understanding hydrothermal dechlorination of PVC by focusing on the operating conditions and hydrochar characteristics. Appl Sci 2017; 7(3):256.

[26] Xiu F R, Wang Y, Yu X, Li Y, Lu Y, Zhou K, et al. A novel safety treatment strategy of DEHP-rich flexible polyvinyl chloride waste through low-temperature critical aqueous ammonia treatment. Sci Total Environ 2020; 708:134532.

[27] Zhao P, Li T, Yan W, Yuan L. Dechlorination of PVC wastes by hydrothermal treatment using alkaline additives. Environ Technol 2018; 39(8):977-985.

[28] Jaksland C, Rasmussen E, Rohde T. A new technology for treatment of PVC waste. J Waste Manag 2000; 20(5-6):463-467.

[29] Wei Y, Fakudze S, Zhang Y, Ma R, Shang Q, Chen J, Liu C, Chu, Q. Co-hydrothermal carbonization of pomelo peel and PVC for production of hydrochar pellets with enhanced fuel properties and dechlorination. Energy 2022, 239:122350.

[30] Xiu F R, Yu X, Qi Y. A high-efficiency and low-temperature subcritical water dechlorination strategy of polyvinyl chloride using coal fly ash (CFA) and coal gangue (CG) as enhancers. J Clean Prod 2020; 260:121085.

[31] Ning X, Dang H, Xu R, Wang G, Zhang J, Zhang N, Wang, C. Co-hydrothermal carbonization of biomass and PVC for clean blast furnace injection fuel production: Experiment and DFT calculation. Renew Energy 2022, 187:156-168.

[32] Li Z, Niu S, Liu J, Wang Y. Solid fuel production from co-hydrothermal carbonization of polyvinyl chloride and corncob: Higher dechlorination efficiency and process water recycling. Sci Total Environ 2022, 843:157082.

[33] Zhao P, Li Z, Li T, Yan W, Ge S. The study of nickel effect on the hydrothermal dechlorination of PVC. J Clean Prod 2017; 152:38-46.

[34] Hashimoto K, Suga S, Wakayama Y, Funazukuri T. Hydrothermal dechlorination of PVC in the presence of ammonia. J Mater Sci 2008; 43(7):2457-2462.

[35] Ma D, Liang L, Hu E, Chen H, Wang D, He C, et al. Dechlorination of polyvinyl chloride by hydrothermal treatment with cupric ion. Process Saf Environ Prot 2021; 146:108-117.

[36] Choma J, Marszewski M, Osuchowski L, Jagiello J, Dziura A, Jaroniec M. Adsorption properties of activated carbons prepared from waste CDs and DVDs. ACS Sustain Chem Eng 2015; 3(4):733-742.

[37] Sun H, La P, Yang R, Zhu Z, Liang W, Yang B, et al. Innovative nanoporous carbons with ultrahigh uptakes for capture and reversible storage of CO_2 and volatile iodine. J Hazard Mater 2017; 321:210-217.

[38] Idrees M, Rangari V, Jeelani S. Sustainable packaging waste-derived activated carbon for carbon dioxide capture. J CO_2 Util 2018; 26:380-387.

[39] Yuan X, Li S, Jeon S, Deng S, Zhao L, Lee K B. Valorization of waste polyethylene terephthalate plastic into N-doped microporous carbon for CO_2 capture through a one-pot synthesis. J Hazard Mater 2020; 399:123010.

[40] Wang J, Wang F, Duan H, Li Y, Xu J, Huang Y, et al. Polyvinyl Chloride-Derived Carbon Spheres for CO_2 Adsorption. ChemSusChem 2020; 13(23):6426-6432.

[41] Liu X, Yang F, Li M, Wang S, Sun C. From polyvinyl chloride waste to activated carbons: the role of occurring additives on porosity development and gas adsorption properties. Sci Total Environ 2022; 833:154894.

[42] Serafin J, Narkiewicz U, Morawski A W, Wrobel R J, Michalkiewicz B. Highly microporous activated carbons from biomass for CO_2 capture and effective micropores at different conditions. J CO_2 Util 2017; 18:73-79.

[43] Travis W, Gadipelli S, Guo Z. Superior CO_2 adsorption from waste coffee ground derived carbons. RSC Adv 2015; 5(37):29558-29562.

[44] Liu J, Sun N, Sun C, Liu H, Snape C, Li K, et al. Spherical potassium intercalated

activated carbon beads for pulverised fuel CO_2 post-combustion capture. Carbon 2015; 94:243-255.

[45] Wei H, Deng S, Hu B, Chen Z, Wang B, Huang J, et al. Granular bamboo-derived activated carbon for high CO_2 adsorption: the dominant role of narrow micropores. ChemSusChem 2012; 5(12):2354-2360.

[46] Li J, Michalkiewicz B, Min J, Ma C, Chen X, Gong J, et al. Selective preparation of biomass-derived porous carbon with controllable pore sizes toward highly efficient CO_2 capture. Chem Eng J 2019; 360:250-259.

[47] Zhang Z, Luo D, Lui G, Li G, Jiang G, Cano Z P, et al. In-situ ion-activated carbon nanospheres with tunable ultramicroporosity for superior CO_2 capture. Carbon 2019; 143:531-541.

[48] Parshetti G K, Chowdhury S, Balasubramanian R. Biomass derived low-cost microporous adsorbents for efficient CO_2 capture. Fuel 2015; 148:246-254.

[49] Yang P, Rao L, Zhu W, Wang L, Ma R, Chen F, et al. Porous carbons derived from sustainable biomass via a facile one-step synthesis strategy as efficient CO_2 adsorbents. Ind Eng Chem Res 2020; 59(13):6194-6201.

[50] Zhao Z, Ma C, Chen F, Xu G, Pang R, Qian X, et al. Water caltrop shell-derived nitrogen-doped porous carbons with high CO_2 adsorption capacity. Biomass Bioenergy 2021; 145:105969.

[51] Liu X, Sun Y, Liu J, Sun C, Liu H, Xue Q, et al. Potassium and zeolitic structure modified ultra-microporous adsorbent materials from a renewable feedstock with favorable surface chemistry for CO_2 capture. ACS Appl Mater Interfaces 2017; 9(32):26826-26839.

[52] Ashourirad B, Arab P, Islamoglu T, Cychosz K A, Thommes M, El-Kaderi H M. A cost-effective synthesis of heteroatom-doped porous carbons as efficient CO_2 sorbents. J Mater Chem A 2016; 4(38):14693-14702.

[53] Rao L, Liu S, Wang L, Ma C, Wu J, An L, et al. N-doped porous carbons from low-temperature and single-step sodium amide activation of carbonized water chestnut shell with excellent CO_2 capture performance. Chem Eng J 2019;

359:428-435.

[54] Rehman A, Heo Y J, Nazir G, Park S J. Solvent-free, one-pot synthesis of nitrogen-tailored alkali-activated microporous carbons with an efficient CO_2 adsorption. Carbon 2021; 172:71-82.

[55] Demir M, Tessema T D, Farghaly A A, Nyankson E, Saraswat S K, Aksoy B, et al. Lignin-derived heteroatom-doped porous carbons for supercapacitor and CO_2 capture applications. Int J Energy Res 2018; 42(8):2686-2700.

[56] Yuan H, Chen J, Li D, Chen H, Chen Y. 5 Ultramicropore-rich renewable porous carbon from biomass tar with excellent adsorption capacity and selectivity for CO_2 capture. Chem Eng J 2019; 373:171-178.

[57] Zhang P, Zhong Y, Ding J, Wang J, Xu M, Deng Q, et al. A new choice of polymer precursor for solvent-free method: Preparation of N-enriched porous carbons for highly selective CO_2 capture. Chem Eng J 2019; 355:963-973.

[58] Qezelsefloo E, Khalili S, Jahanshahi M, Peyravi M. Adsorptive removal of CO_2 on Nitrogen-doped porous carbon derived from polyaniline: Effect of chemical activation. Mater Chem Phys 2020; 239:122304.

Graphical abstract